Magnetic properties of the antiferromagnetic double perovskite Ba$_2$PrRuO$_6$

Magnetic properties of the antiferromagnetic double perovskite Ba$_2$PrRuO$_6$

Yuki Izumiyama[1]**, Yoshihiro Doi**[1]**, Makoto Wakeshima**[1]**, Yukio Hinatsu**[1]**, Yutaka Shimojo**[2] **and Yukio Morii**[2]

[1] Division of Chemistry, Graduate School of Science, Hokkaido University, Sapporo 060-0810, Japan
[2] Japan Atomic Energy Research Institute, Tokai-mura, Ibaraki 319-1195, Japan

Abstract

The ordered perovskite compound Ba$_2$PrRuO$_6$ is prepared and its magnetic properties are investigated. The Rietveld analysis of the neutron diffraction profiles measured at 150 K shows that the Pr^{3+} and Ru^{5+} ions are arranged with regularity over the six-coordinate B sites of the perovskite ABO$_3$ and that Ba$_2$PrRuO$_6$ belongs to space group $P2_1/n$, with $a = 6.0063(5)$, $b = 5.9863(4)$, $c = 8.4677(7)$ Å and 90.04(2)°. The magnetic susceptibility and the heat capacity measurements show that this compound transforms to an antiferromagnetic state below 117 K. From the neutron diffraction patterns measured at 7 K, the magnetic structure is determined to be of Type I and the magnetic moments of Pr^{3+} and Ru^{5+} are estimated to be 2.2(1) and 2.0(2) μ_B, respectively. Their values are discussed on the basis of theoretical calculations for the crystal field splitting.

1. Introduction

Ordered perovskite-type oxides A$_2$LnMO$_6$ (A = alkaline earth elements; Ln = rare earth elements; M = 4d or 5d transition elements) in which the Ln and M elements regularly order, show a variety of magnetic behaviour at low temperatures. The electronic structure of Ru^{5+} is [Kr]4d^3 ([Kr]: krypton core). Such highly oxidized cations from the second transition series sometimes show quite unusual magnetic behaviour. When the Ln ion is diamagnetic (e.g. Y^{3+}, La^{3+} and Lu^{3+}), such A$_2$LnRuO$_6$ compounds are suitable to study the behaviour of Ru^{5+} ions because only the Ru^{5+} ions are responsible for their magnetic properties [1–3]. Most of these compounds show antiferromagnetic transitions at 15–30 K.

The effective magnetic moments (μ_{eff}) of Ru^{5+} ions are also complicated. The moments of 3.84–4.27 μ_B are reported for Ca$_2$LnRuO$_6$ (Ln = Y, La), Ba$_2$LaRuO$_6$ [1] and BaLaMRuO$_6$ (M = Mg, Zn) [4], which are very close to the spin-only value of 3.87 μ_B for the t$_{2g}^3$ configuration. In the octahedrally coordinated Ru^{5+}: 4d^3 ions, any orbital contribution is expected to reduce the effective magnetic moment from the spin-only value, and the Ru^{5+} ion

should have a μ_{eff} of about 3.50 μ_B [5]. Some Ru^{5+} compounds with the general formula M^1RuF_6 have μ_{eff} values ranging from 3.48 to 3.70 μ_B [5].

In this study, we have selected the praseodymium ion as the Ln in the A_2LnRuO_6. This praseodymium ion has the tetravalent state in addition to the trivalent state which is the common oxidation state for the lanthanides. When the tetravalent praseodymium ions are accommodated at the B sites of the perovskite-type oxides ABO_3, some interesting magnetic cooperative phenomena are observed at low temperatures. Barium praseodymium oxide $BaPrO_3$ shows an antiferromagnetic transition at 11.6 K. A very sharp drop in the susceptibility is observed when the temperature is increased through the transition temperature [6, 7]. When the praseodymium ion is accommodated in an ordered perovskite-type oxide, Ba_2PrIrO_6, an antiferromagnetic transition has been observed at a relatively high temperature 71 K. It is discussed that this high transition temperature is due to the magnetic interactions between 4f electrons of praseodymium ions and 5d electrons of iridium ions [8]. Therefore, some unique magnetic properties are expected for the oxides having both d and f electrons, and we have been greatly interested in the ordered perovskites A_2PrRuO_6. Doi *et al* pointed out that it was difficult to prepare Sr_2LnRuO_6 (Ln = La–Pr) because of the large sizes of the Ln ions compared with that of the Sr^{2+} ion [9].

In this study, we have paid attention to a compound Ba_2PrRuO_6 in which both the praseodymium and ruthenium ions are accommodated in the B sites of the perovskite, and have investigated its magnetic properties through measurements of the magnetic susceptibility, heat capacity and powder neutron diffraction. In addition, we have determined the octahedral crystal field energy level for the Pr ion in Ba_2PrRuO_6 from the temperature dependence of the magnetic susceptibilities for an isostructural ordered perovskite Ba_2PrTaO_6 [10].

2. Experiment

A polycrystalline sample of Ba_2PrRuO_6 was synthesized by heating the stoichiometric amounts of $BaCO_3$, Pr_6O_{11} and RuO_2, first at 1173 K for 12 hours and then 1473 K for 72 hours, in air with frequent grindings and pelletings. The progress of the reactions was monitored by the powder x-ray diffraction measurements with a Rigaku RINT 2100 diffractometer using Cu Kα radiation. Powder neutron diffraction measurements were performed at 150 K and 7 K using a high resolution powder diffractometer (HRPD) at the JRR-3M reactor (Japan Atomic Energy Research Institute), with a Ge(331) monochromator ($\lambda = 1.8230$ Å). The collimators used were 6′–20′–6′, which were placed before and after the monochromator, and between the sample and each detector. The set of 64 detectors and collimators, which were placed every 2.5 degrees, rotates around the sample. All the data collected by x-ray and neutron diffraction measurements were analysed by the Rietveld technique using the program RIETAN [11], and both crystal and magnetic structures were determined.

The magnetic susceptibility was measured in the temperature range of 2–300 K in a magnetic field of 0.1 T with a SQUID magnetometer (Quantum Design, model MPMS). The susceptibility data were collected after cooling the sample from room temperature to 2 K in a zero field (ZFC) and after cooling it in the applied field (FC). The field dependence of magnetization was measured at 1.8 K over the applied magnetic field range $-5\,T \leqslant H \leqslant 5\,T$.

The heat capacity measurements were carried out using a relaxation technique supplied by the commercial heat capacity measurement system (Quantum Design, model PPMS) in the temperature range from 2 to 300 K. The sample in the form of a pellet ($\sim$10 mg) was mounted on an alumina plate with apiezon for better thermal contact.

3. Results and discussion

3.1. Crystal structure

The powder x-ray diffraction measurements show that Ba$_2$PrRuO$_6$ was formed as a single phase with a perovskite-type structure. Among the analogous perovskite compounds Ba$_2$LnRuO$_6$ (Ln = La, Nd, Lu), Ba$_2$NdRuO$_6$ adopts monoclinic symmetry in space group $P2_1/n$ [12], while Ba$_2$LaRuO$_6$ has triclinic symmetry in space group $P\bar{1}$ [1] and Ba$_2$LuRuO$_6$ is cubic with space group $Fm3m$ [2]. These space groups all permit an NaCl-type ordered arrangement of Ln^{3+} and Ru^{5+} ions. The diffraction data of Ba$_2$PrRuO$_6$ were analysed by the Rietveld profile analysis technique. The diffraction pattern could be indexed on a monoclinic unit cell, in space group $P2_1/n$, which gave the best refinement in the calculation based on the other space groups. In this compound, Pr and Ru ions are located at $2d(1/2, 0, 0)$ and $2c(1/2, 0, 1/2)$ sites, respectively, and their occupation factors were determined to be both one. The model assuming that the Pr and Ru ions (partially) randomly located at $2d$ and $2c$ sites gave much poorer calculation results. Figure 1 shows the crystal structure of Ba$_2$PrRuO$_6$, indicating that the Pr and Ru cations form two interpenetrating face-centred sublattice unit cells. Refinements of the profile parameters and the atomic positional parameters have led to the reliability factors, $R_{wp} = 12.03$, $R_I = 1.50$ and $R_F = 3.20\%$, and the lattice parameters converged are $a = 6.0069(4)$, $b = 5.9930(4)$, $c = 8.4912(8)$ Å and $\beta = 90.04(1)°$.
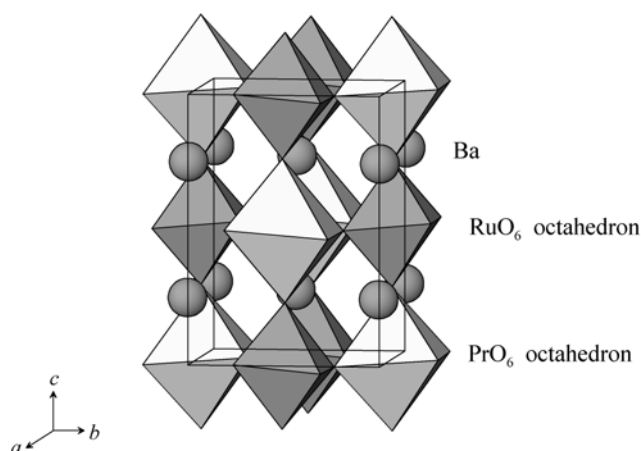

Figure 1. The crystal structure of Ba$_2$PrRuO$_6$. Spheres are Ba atoms, light octahedra are PrO$_6$ units and dark octahedra are RuO$_6$ units.

The praseodymium ion adopts the tetravalent state as well as the trivalent state. It so far has been reported that the Ln and Ru ions are trivalent and pentavalent, respectively, in analogous compounds Ba$_2$LnRuO$_6$ (Ln = La–Eu) [1, 13, 14]. The variation of lattice parameters with the ionic Ln^{3+} radius from La to Eu is shown in figure 2, where they are found to increase monotonically with the ionic radius of the Ln^{3+} ion with no deviation from the trend. This result is unlike the case of the tetravalent Pr and Ir ions in Ba$_2$PrIrO$_6$ in a series of Ba$_2$LnIrO$_6$ [8], and obviously indicates the trivalent Pr and pentavalent Ru ions in this compound.
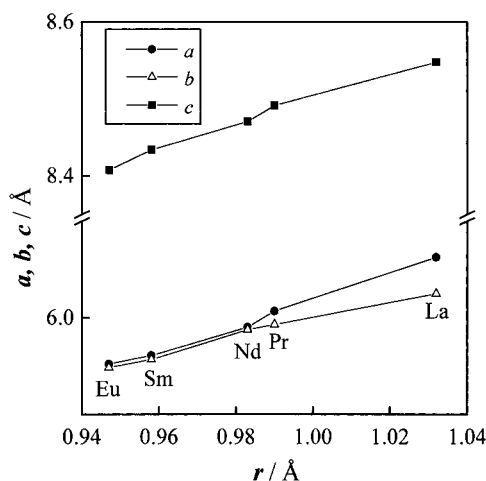
Figure 2. Variation of lattice parameters for Ba_2LnRuO_6 (Ln = La–Eu) with the ionic radius of Ln^{3+}.

3.2. Magnetic properties

The temperature dependence of the molar magnetic susceptibilities for Ba_2PrRuO_6 is shown in figure 3. A magnetic anomaly has been found at 117 K. Below this temperature, no divergence between the ZFC and FC magnetic susceptibilities occur. This Ba_2PrRuO_6 has the highest magnetic transition temperature in a family of A_2LnRuO_6 [1–3]. By fitting the Curie–Weiss equation to the experimental data in the temperature range between 200 and 300 K, the effective magnetic moment (μ_{eff}) and the Weiss constant (θ) are determined to be 5.24 μ_B and −133 K, respectively. This negative Weiss constant is indicative of the presence of predominant antiferromagnetic interaction. No divergence between the ZFC and the FC magnetic susceptibilities or no magnetic hysteresis in the magnetization–magnetic field curve

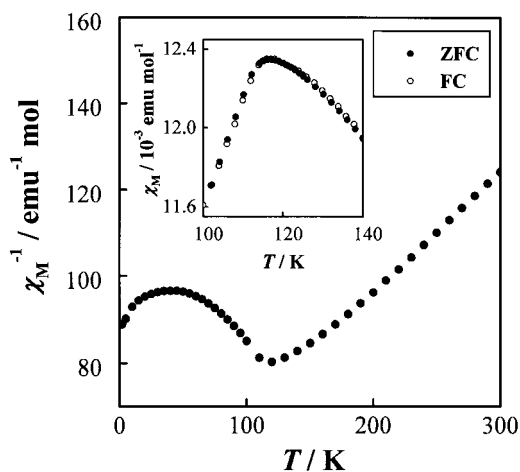**Figure 3.** The reciprocal magnetic susceptibilities of Ba_2PrRuO_6 against temperature. Inset shows the temperature dependence of the magnetic susceptibilities, where the ZFC (filled symbols) and FC (open symbols) are molar magnetic susceptibilities for Ba_2PrRuO_6 in the applied field of 0.1 T.

indicate that below 117 K this compound transforms to an antiferromagnetic state without weak ferromagnetic properties. Both the Pr^{3+} and Ru^{5+} ions contribute to the paramagnetic behaviour of Ba$_2$PrRuO$_6$, and the effective magnetic moment of this compound (μ_{eff}) is given by the following equation: $\mu_{eff}^2 = \mu_{eff}(\text{Pr}^{3+})^2 + \mu_{eff}(\text{Ru}^{5+})^2$. Since the theoretical moment of the Pr^{3+} ions is 3.58 μ_B, the magnetic moment for the Ru^{5+} ion is estimated to be 3.83 μ_B, which is rather close to the spin-only value 3.87 μ_B for the d^3 electron configuration. For 4d transition metal ions, a spin–orbit coupling should be considered and they are expected to have the effective magnetic moments which are reduced from spin-only value 3.87 μ_B by the factor $(1 - \alpha\lambda/10Dq)$, where α is 4 for the A$_2$ ground term and the spin–orbit coupling constant λ has a value of 500 cm^{-1} for Ru^{5+} [4, 5], i.e. the relation is given as follows:

$$\mu_{eff} = \mu_{spin\text{-}only}\left(1 - \alpha\frac{\lambda}{10Dq}\right). \tag{1}$$

The Ru^{5+} ion should have a μ_{eff} of about 3.50 μ_B from the above equation. The effective magnetic moment experimentally obtained is closer to the spin-only value 3.87 μ_B than the value taking into account the spin–orbit interaction, 3.50 μ_B. The octahedral crystal field splits the fivefold-degenerate d orbitals into t$_{2g}$ and e$_g$ orbitals, and three electrons of the Ru^{5+} ion occupy the t$_{2g}$ orbitals. This t$_{2g}^3$ electron configuration in the ideal octahedral crystal field has an almost quenched orbital angular momentum. Comparable effective magnetic moments of Ru^{5+} ions are reported for the compounds with the general formula A$_2$BRu^{V}O$_6$ (A = Ba, B = Y, La, Lu) which have μ_{eff} values ranging from 4.00 to 4.50 μ_B [1, 2].

3.3. Heat capacity

Figure 4 shows the temperature dependence of the heat capacity for Ba$_2$PrRuO$_6$. The λ-type anomaly has been observed at 117 K, which corresponds to the antiferromagnetic transition measured in the magnetic susceptibility versus temperature curve and indicates the existence of a second order phase transition.
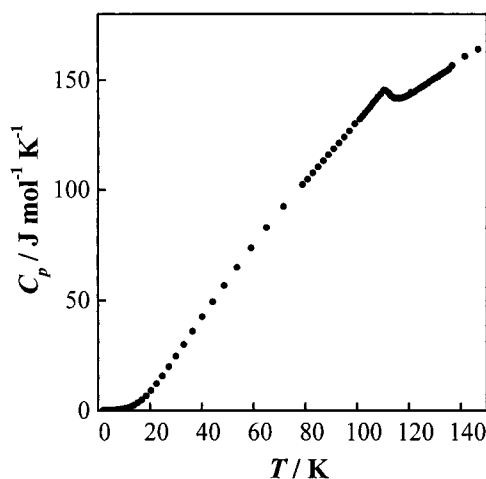

Figure 4. Temperature dependence of the heat capacity of Ba$_2$PrRuO$_6$.

3.4. Neutron diffraction measurements

Figure 5 shows the enlarged powder neutron diffraction patterns measured at 150 and 7 K. The neutron diffraction data collected at 150 K could well be refined with the space group $P2_1/n$, which is, of course, in agreement with the result by the x-ray diffraction measurements. The lattice parameters and the atomic positions thus determined are listed in table 1. The reliability factors are $R_{wp} = 9.89$, $R_I = 2.09$ and $R_F = 1.64\%$. Some selected bond lengths and bond angles are listed in table 2. The Ru–O bond lengths are almost equal to those in various Ru^{5+} compounds [1–3] and are shorter than those in Ru^{4+} compounds, for example in $BaRuO_3$ [15]. The O–Pr–O bond angles are approximately equal and they are nearly $90°$. The same situation is valid for the bond angles of O–Ru–O, that is, both the Pr^{3+} ions and Ru^{5+} ions are in an almost octahedral environment by six oxygen ions. This result verifies our discussion that the effective magnetic moment for the Ru^{5+} ion in Ba_2PrRuO_6 can be described as the spin-only value because an ideal octahedral environment has the t_{2g}^3 orbital angular momentum for the Ru^{5+} ions quenched. It is worthy of note that the bond length Pr–O(1) is larger than the bond length Pr–O(2) at 150 K and this relation is reversed when the temperature is 7 K. A similar situation is found in the bond lengths of Ru–O(1) and Ru–O(2), and in the bond angles of Pr–O(1)–Ru and Pr–O(2)–Ru (see table 2).

The neutron diffraction data collected at 7 K show a number of low angle peaks which

Table 1. Structural parameter for Ba_2PrRuO_6 (space group $P2_1/n$).

Atoms	Site	x	y	z	B (Å^2)	$\mu(\mu_B)$
At 150 K						
Ba	4e	−0.000(4)	−0.007(4)	0.248(4)	0.14(9)	
Pr	2d	1/2	0	0	0.22(7)	
Ru	2c	1/2	0	1/2	0.22(7)	
O(1)	4e	0.224(3)	0.274(5)	0.018(2)	0.53(7)	
O(2)	4e	0.236(3)	−0.267(5)	0.010(2)	0.53(7)	
O(3)	4e	−0.037(3)	0.500(3)	0.232(2)	0.53(7)	
$a = 6.0063(5)$ Å $b = 5.9863(4)$ Å $c = 8.4677(7)$ Å $\beta = 90.04(2)°$						
$V = 304.46(4)$ Å^3 $R_{WP} = 9.89\%$ $R_I = 2.09\%$ $R_F = 1.64\%$ $R_e = 6.91\%$						
At 7 K						
Ba	4e	−0.002(2)	0.002(3)	0.249(3)	0.03(7)	
Pr	2d	1/2	0	0	0.1(1)	2.2(1)
Ru	2c	1/2	0	1/2	0.1(1)	2.0(2)
O(1)	4e	0.236(2)	0.268(4)	0.012(2)	0.2(8)	
O(2)	4e	0.224(3)	−0.274(4)	0.021(2)	0.2(8)	
O(3)	4e	−0.039(2)	0.490(3)	0.231(1)	0.2(8)	
$a = 6.0079(5)$ Å $b = 5.9841(4)$ Å $c = 8.4524(6)$ Å $\beta = 90.07(1)°$						
$V = 303.88$ Å^3 $R_{WP} = 11.29\%$ $R_I = 2.37\%$ $R_F = 1.77\%$ $R_e = 7.14\%$						

Definitions of reliability factors R_{WP}, R_I, R_F and R_e are given as follows:

$$R_{WP} = \left[\sum w(|F(o)| - |F(c)|)^2 \Big/ \sum w|F(o)|^2 \right]^{1/2}$$

$$R_I = \sum |I_k(o) - I_k(c)| \Big/ \sum I_k(o)$$

$$R_F = \sum |[I_k(o)]^{1/2} - [I_k(c)]^{1/2}| \Big/ \sum [I_k(o)]^{1/2}$$

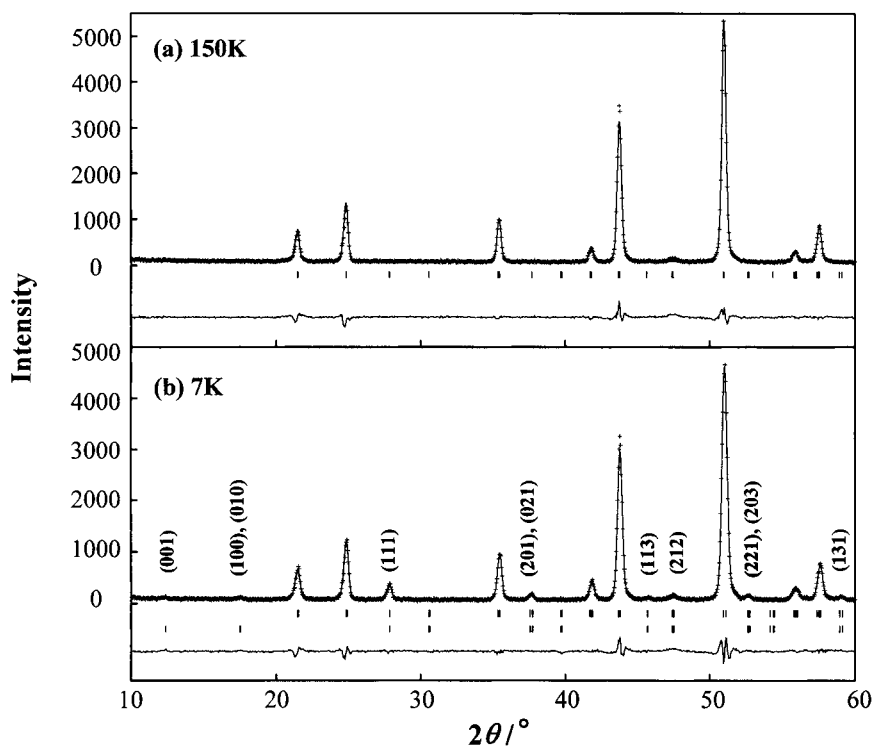$$R_e = \left(\frac{N - p}{\sum_i w_i y_i^2} \right)^{1/2}.$$

Figure 5. Enlarged powder neutron diffraction patterns for Ba$_2$PrRuO$_6$ at 150 K (*a*) and 7 K (*b*). The calculated and observed profiles are shown on the top solid line and cross markers, respectively. The vertical marks in the middle show positions calculated for Bragg reflections. In (*b*), the nuclear reflection positions are shown as upper vertical marks and magnetic ones are shown as lower ones. The lower trace is a plot of the difference between calculated and observed intensities.

Table 2. Bond lengths (in Å) and bond angles (degrees) for Ba$_2$PrRuO$_6$.

At 150 K						
Pr–O(1)	2.34(2) Å × 2			Ru–O(1)	1.91(2) Å × 2	
Pr–O(2)	2.25(2) Å × 2			Ru–O(2)	1.97(2) Å × 2	
Pr–O(3)	2.29(2) Å × 2			Ru–O(3)	1.99(2) Å × 2	
O(1)–Pr–O(2)	89.8(8)°	O(1)–Ru–O(2)	90.5(9)°	Pr–O(1)–Ru	172(1)°	
O(1)–Pr–O(3)	90.3(8)°	O(1)–Ru–O(3)	90.1(8)°	Pr–O(2)–Ru	175(1)°	
O(2)–Pr–O(3)	89.9(5)°	O(2)–Ru–O(3)	90.7(3)°	Pr–O(3)–Ru	168(1)°	
At 7 K						
Pr–O(1)	2.26(2) Å × 2			Ru–O(1)	1.98(2) Å × 2	
Pr–O(2)	2.34(2) Å × 2			Ru–O(2)	1.92(2) Å × 2	
Pr–O(3)	2.29(2) Å × 2			Ru–O(3)	1.96(2) Å × 2	
O(1)–Pr–O(2)	90.2(8)°	O(1)–Ru–O(2)	90.8(9)°	Pr–O(1)–Ru	174(1)°	
O(1)–Pr–O(3)	92.5(8)°	O(1)–Ru–O(3)	90.7(8)°	Pr–O(2)–Ru	170(1)°	
O(2)–Pr–O(3)	91.4(5)°	O(2)–Ru–O(3)	90.7(3)°	Pr–O(3)–Ru	167(1)°	

were not observed at 150 K, indicating that this compound exhibits long-range magnetic ordering at low temperatures. At 7 K, Ba$_2$PrRuO$_6$ has the same crystal structure as that at 150 K. In the analysis of the neutron diffraction data measured at 7 K, we assumed that

all the magnetic moments were collinear since no magnetic satellite reflections exist. In addition, the size of the magnetic unit cell is as large as that of the crystal unit cell, since there appeared no superlattice reflections, and thus the magnetic unit cell is described as $a \approx \sqrt{2} a_p$, $b \approx \sqrt{2} a_p$, $c \approx 2 a_p$, where a_p means a lattice parameter in a primitive cubic perovskite unit cell. Reflection conditions for the space group $P2_1/n$ are as follows:

$(h\,0\,l)$	$h + l = 2n$
$(0\,k\,0)$	$k = 2n$
$(h\,0\,0)$	$h = 2n$
$(0\,0\,l)$	$l = 2n$

(n: arbitrary integer).

The magnetic reflections observed at 7 K can be indexed simply with the condition that $[h + k + l]$ is an odd integer. Three types of antiferromagnetic magnetic structure are known for such perovskite compounds in which magnetic ions at the B sites form a face centred array, that is, Types I, II and III. In the case of identical magnetic ions, we consider two principal magnetic superexchange interactions between nearest-neighbour (NN) magnetic ions separated by a distance of $\sqrt{2} a_p$, and between next-nearest-neighbour (NNN) magnetic ions separated by a distance of $2 a_p$. Type I is defined as the antiferromagnetic magnetic structure in which interactions of NN and NNN magnetic ions are antiferromagnetic and ferromagnetic, respectively [2]. Type II and Type III are more complicated, and their magnetic unit cells are eight times and twice as large as that of the crystal unit cell, respectively. Type I where the magnetic structure has the same size as that of the crystal unit cell is the only magnetic structure for the present case, and thus the following magnetic sites are available:

Position	x	y	z
Pr1	0	1/2	1/2
Pr2	1/2	0	0
Ru1	0	1/2	0
Ru2	1/2	0	1/2

The magnetic moments of Pr1 and Pr2 are antiparallel with each other, and those of Ru1 and Ru2 are also antiparallel with each other. Their respective magnetic moments are defined as S_{Pr1}, S_{Pr2}, S_{Ru1} and S_{Ru2}.

The magnetic structure factor $F_m(h\,k\,l)$ for an $(h\,k\,l)$ reflection is defined by the following equation:

$$F_m = \sum_j |q_j| b_{mj} \exp[2\pi i (hx_j + ky_j + lz_j)] \tag{2}$$

with

$$q = e(e \cdot s) - s \qquad (|q_i| = q_i) \tag{3}$$

where b_m is the magnetic scattering amplitude, vector e is the unit scattering vector and s is the unit vector parallel to the magnetic moments. In this case, the magnetic structure factor is given in the following:

$$F_m = q_{Pr1} b_{Pr1} \{\exp[i\pi(k + 1)]\} + q_{Pr2} b_{Pr2} \{\exp[i\pi h]\} + q_{Ru1} b_{Ru1} \{\exp[i\pi k]\}$$
$$+ q_{Ru2} b_{Ru2} \{\exp[i\pi(h + 1)]\}. \tag{4}$$

In the case of the antiferromagnetic structure, the relations $q_{Pr1} b_{Pr1} = -q_{Pr2} b_{Pr2}$ and $q_{Ru1} b_{Ru1} = -q_{Ru2} b_{Ru2}$ hold. Therefore, the magnetic structure factors for the magnetic Bragg reflections (100), (010) and (001) are calculated to be the following;

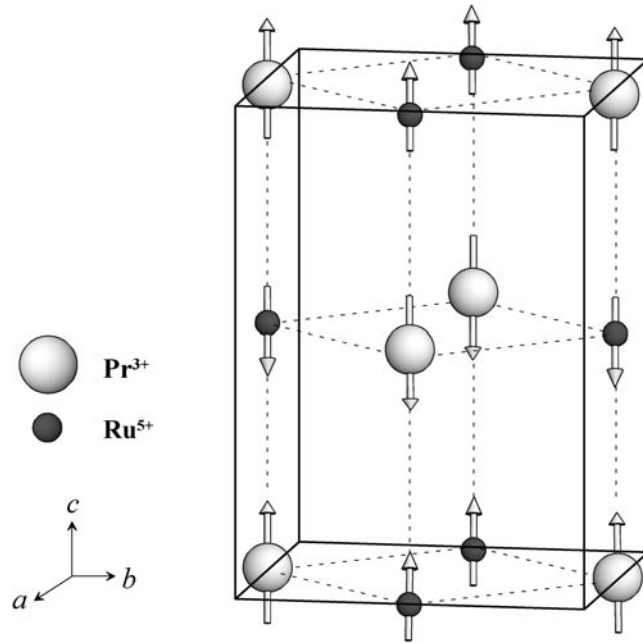$$F_m(100) = 2(q_{Pr1} b_{Pr1} + q_{Ru1} b_{Ru1}) \tag{5}$$

Figure 6. The magnetic structure of Ba$_2$PrRuO$_6$. Diamagnetic ions are omitted. Larger circles Pr^{3+}; smaller circles Ru^{5+}.

$$F_m(010) = -2(q_{Pr1}b_{Pr1} + q_{Ru1}b_{Ru1}) \tag{6}$$

$$F_m(001) = -2(q_{Pr1}b_{Pr1} - q_{Ru1}b_{Ru1}). \tag{7}$$

Experimental results (figure 5(b)) show that the magnetic reflections of (100) or (010) planes have some intensity and that the intensity of the (001) plane is actually null. Therefore, the above equations (5)–(7) are $F_m(100) \neq 0$, $F_m(010) \neq 0$ and $F_m(001) \approx 0$, respectively. Here in order to satisfy $F_m(001) \approx 0$, two possibilities are considered.

The first case is that both the magnetic moments S_{Pr1} and S_{Ru1} have nearly equal magnitudes and they are parallel with each other. The second case is that the alignment of the magnetic moments is perpendicular to the (001) planes, i.e. they are parallel to the c-axis.

The theoretical moments of the free Pr^{3+} ion (4f^2 electronic configuration) and the Ru^{5+} ion (4d^3 electronic configuration) are 3.2 μ_B and 3.0 μ_B, respectively, i.e. they are comparable with each other. If the moments S_{Pr1} and S_{Ru1} are parallel, $F_m(001)$ becomes zero. At the same time, both $F_m(100)$ and $F_m(010)$ have some values and the magnetic reflections of (100) or (010) planes should be observed strongly. However, they were observed with weak intensities in the neutron diffraction pattern (see figure 5(b)). This result means that it is essential that S_{Pr1} and S_{Ru1} should be antiparallel with each other. Thus the first case is not appropriate for this, and we consider that the second possibility is reasonable, i.e. the alignment of the magnetic moments is parallel to the c-axis.

Then we have performed the Rietveld analysis using a program RIETAN and succeeded in determining the magnetic structure. The magnetic moments are calculated to be 2.2(1) μ_B for Pr^{3+} and 2.0(2) μ_B for Ru^{5+}. The structural and magnetic parameters refined are tabulated in table 1, and the reliability factors are $R_{wp} = 11.29$, $R_I = 2.37$ and $R_F = 1.77\%$. The magnetic structure for Ba$_2$PrRuO$_6$ determined is illustrated in figure 6. In this case of Type I, both the

magnetic moments of the Pr^{3+} and Ru^{5+} ions which exist on the *ab*-plane are aligned along the *c*-axis direction, therefore the *ab*-planes would be ferromagnetic planes. The ferromagnetic *ab*-planes are stacked antiferromagnetically along the *c*-axis.

The magnetic moment of the Pr^{3+} ion determined from the analysis of the neutron diffraction data (2.2(1) μ_B) is smaller than the theoretical value for the free Pr^{3+} ion, 3.2 μ_B by about 1.0 μ_B. In the Ba_2PrRuO_6, where the Pr ions are surrounded by six-coordinate oxygen ions, the cubic crystalline electric field splits the ninefold-degenerate ground state multiplet $^3H_4$ of the Pr^{3+} ion into a singlet Γ_1, a doublet Γ_3, and two triplets Γ_4 and Γ_5 [16]. The octahedral crystal field energy-level for the Pr^{3+} ion is derived from the temperature dependence of the magnetic susceptibilities for Ba_2PrTaO_6. The ground state is Γ_1, and the first and second exited states are Γ_4 and Γ_3, respectively. The energy of the $\Gamma_1 \rightarrow \Gamma_4$ transition is 550 K and that of $\Gamma_1 \rightarrow \Gamma_3$ is 880 K [10]. The value of magnetic moment is zero from the ground state of the Pr^{3+} (a singlet Γ_1), while since the Pr^{3+} ion in Ba_2PrRuO_6 brings about the magnetic ordering at a relative high temperature 112 K, the $\Gamma_1 \rightarrow \Gamma_4$ transition needs to be considered. The wavefunctions for Γ_1 and Γ_4 are given as follows, respectively [16]:

$$\Gamma_1 : \sqrt{5/24}|4\rangle + \sqrt{7/12}|0\rangle + \sqrt{5/24}|-4\rangle \tag{8}$$

$$\Gamma_4 : \begin{cases} \sqrt{1/2}|4\rangle - \sqrt{1/2}|-4\rangle \\ \sqrt{1/8}|\pm3\rangle + \sqrt{7/8}|\mp1\rangle \end{cases} \tag{9}$$

and the expected value of $\boldsymbol{J}_Z$, $\langle\Gamma_1|\boldsymbol{J}_Z|\Gamma_4\rangle$ is calculated to be

$$\langle\Gamma_1|\boldsymbol{J}_Z|\Gamma_4\rangle = \sqrt{5/24} \times \sqrt{1/2} \times 4 + \sqrt{5/24} \times (-\sqrt{1/2}) \times (-4) = 2.58. \tag{10}$$

Hence the theoretical magnetic moment is calculated to be 2.07 μ_B with the g_J value for the Pr^{3+} ion, 4/5. This value is comparable with the ordered magnetic moment determined from the Rietveld analysis for the powder neutron diffraction measurements at 7 K. The reason why the value of magnetic moment of Pr^{3+} ion in Ba_2PrRuO_6 is not saturated with 3.2 μ_B even at 7 K (2.2(1) μ_B) is rationalized from considering the multiple states split by the crystalline electric field.

On the other hand, the ordered magnetic moment of the Ru^{5+} ion in Ba_2PrRuO_6 is determined to be 2.0(2) μ_B, which is smaller than the value expected for the d^3 electronic configuration (3.0 μ_B). This reduction of the Ru^{5+} moment may be attributed to thermal fluctuations and/or covalent effects. We should also notice the fact that the form factor for Zr^+ given in *The International Tables for Crystallography* [17] has been used for the magnetic intensity calculations because the form factor for Ru^{5+} is not available. Comparable magnetic moments around 2.0 μ_B are reported for many magnetically ordered Ru^{5+} oxides [1–3, 12].

Acknowledgments

References

[1] Battle P D, Goodenough J B and Price R 1983 *J. Solid State Chem.* **46** 234–44
[2] Battle P D and Jones C W 1989 *J. Solid State Chem.* **78** 108–16
[3] Battle P D and Macklin W J 1984 *J. Solid State Chem.* **52** 138–45

[4] Hong K P, Choi Y H, Kwon Y U, Jung D Y, Lee J S, Shim H S and Lee C H 2000 *J. Solid State Chem.* **150** 383–90

[5] Byrne R C and Moeller C W 1970 *J. Solid State Chem.* **2** 228–35

[6] Rosov N, Lynn J W, Lin Q, Cao G, O'Reilly J W, Pernambuco-Wise P and Crow J E 1992 *Phys. Rev.* B **45** 982–6

[7] Hinatsu Y 1995 *J. Solid State Chem.* **119** 405–11

[8] Wakeshima M, Harada D and Hinatsu Y 2000 *J. Mater. Chem.* **10** 419–22

[9] Doi Y and Hinatsu Y 1999 *J. Phys.: Condens. Matter* **11** 4813–20

[10] Doi Y and Hinatsu Y, unpublished results.

[11] Izumi F 1993 *The Rietveld Method* ed R A Young (Oxford: Oxford University Press) ch 13

[12] Izumiyama Y, Doi Y, Wakeshima M, Hinatsu Y, Oikawa K, Shimojo Y and Morii Y 2000 *J. Mater. Chem.* **10** 2364–7

[13] Greatrex R, Greenwood N N, Lal M and Fernandez I 1979 *J. Solid State Chem.* **30** 137–48

[14] Gibb T C and Greatrex R 1980 *J. Solid State Chem.* **34** 279–88

[15] Santoro A, Natali Sora I and Huang Q 2000 *J. Solid State Chem.* **151** 245–52

[16] Lea K R, Leask M J M and Wolf W P 1962 *J. Phys. Chem. Solids* **23** 1381–405

[17] Brown P J 1995 *The International Tables for Crystallography* vol C, ed A J C Wilson (Dordrecht: Kluwer) ch 4